Accurate luminosities for F-G supergiants from FeII/FeI line depth ratios

V. V. Kovtyukh, F. A. Chekhonadskikh, R. E. Luck, C. Soubiran, M. P. Yasinskaya, S. I. Belik

Accurate luminosities for F–G supergiants from Fe II / Fe I line depth ratios

V. V. Kovtyukh,[1,2]★ F. A. Chekhonadskikh,[1,2] R. E. Luck,[3] C. Soubiran,[4]
M. P. Yasinskaya[1,2] and S. I. Belik[1,2]

[1]*Astronomical Observatory, Odessa National University, T. G. Shevchenko Park, 65014, Odessa, Ukraine*
[2]*Isaac Newton Institute of Chile, Odessa Branch, Ukraine*
[3]*Department of Astronomy, Case Western Reserve University, 10900 Euclid Avenue, Cleveland, OH 44106-7215, USA*
[4]*Universit é de Bordeaux - CNRS - Laboratoire d'Astrophysique de Bordeaux, BP 89, 33270 Floirac, France*

ABSTRACT

Luminous FG supergiants can be used as extragalactic distance indicators. In order to fully exploit the properties of these bright stars, we must first learn how to measure their luminosities. Based primarily on classical Cepheids and supergiants in clusters and OB associations, we have derived 80 empirical relations connecting the line depth ratios of Fe II/Fe I lines with the absolute magnitudes M_v and the effective temperatures T_{eff}. These relations have been applied to estimate the absolute magnitudes of 98 FG supergiants with an error of ±0.26 mag. The application range of our calibrations is spectral types F2–G8 and luminosity classes I and II (absolute magnitudes M_v, -0.5 to -8 mag). A comparison of our M_v determinations with values from the literature shows good agreement.

Key words: stars: fundamental parameters – supergiants – stars: variables: Cepheids.

1 INTRODUCTION

Positioning a star in the Hertzsprung–Russell (H–R) diagram is fundamental for understanding its structure and evolution, as it enables a proper comparison with the theoretical evolutionary tracks. FG supergiants are very luminous stars and can be seen up to large distances. However, being rare and residing in the galactic plane, they are normally severely reddened. This presents a serious problem for studying supergiants, in particular when trying to infer their intrinsic luminosities. The Cepheid period–luminosity (PL) relation remains the primary tool for the determination of the distances (and hence luminosities) for the Local Group and other nearby galaxies. The absolute calibration of this relation relies on accurate estimates of the distance of the calibrating Cepheids, and their interstellar extinction and reddening. For supergiants that are not periodic variables, the PL relation is obviously not applicable. Other techniques are needed for the determination of the absolute magnitudes and luminosities of a wide range of supergiants. In this work, we turn to spectroscopy to search for luminosity-sensitive features.

The luminosity classification of F–G stars is primarily based on the line strength ratios between the lines and blends of ionized metals, such as Fe II, Ti II, Sr II, Y II, and the lines and blends of neutral metals (Gray 1992). A quantifying of line ratios as a function of absolute magnitude thus seems a possibility. A number of studies have been dedicated to the determination of the luminosity scale for non-periodic supergiants (see Arellano Ferro, Giridhar & Rojo Arellano

2003 and references therein). Arellano Ferro, Mendoza & Eugenio (1993) presented calibrations of absolute magnitudes for A0–G2 stars based on the strength of the O I 7774 Å lines, narrow-band photometry and low-resolution spectroscopy. These calibrations allow absolute magnitude estimates with a precision of 0.6 mag. The calibrations were further improved in Arellano Ferro et al. (2003) to achieve a precision of 0.38 mag for non-periodic supergiants and about 0.42 mag for Cepheids. This method requires spectra of high signal-to-noise (S/N) ratio at the O I 7774 Å lines, a difficult proposition for distant stars. Another complication is that the O I 7774 feature is sensitive to the oxygen abundance (and microturbulence) with the M_v–W(O I 7774) calibration being determined only for a near-solar oxygen abundance. Similarly, Andrievsky (1998a,b) suggested the use of Ba II lines to calibrate the absolute magnitudes of non-variable supergiants and low-amplitude Cepheids.

The use of colour indices to derive absolute magnitudes allows us to reach fainter objects that lie at larger distances. Arellano Ferro & Parrao (1990) presented a calibration of absolute magnitudes of luminous F–G supergiants using the $uvby\beta$ photometric system. In this study, the calibrators were (hopefully) non-variable yellow supergiants with known extinction and absolute magnitudes. This method, however, also suffers from relatively low precision and is difficult to apply to strongly reddened stars in the galactic plane.

Apart from the O I 7774 Å and Ba II lines, we have noticed other lines in the spectra of supergiants that are sensitive to luminosity. Other lines from first ionized species behave similarly to Ba II. For example, at a given T_{eff} in more luminous supergiants, Fe II lines are stronger than Fe I lines. Fe II lines should therefore be investigated as potential luminosity indicators. The ratio Fe II/Fe I
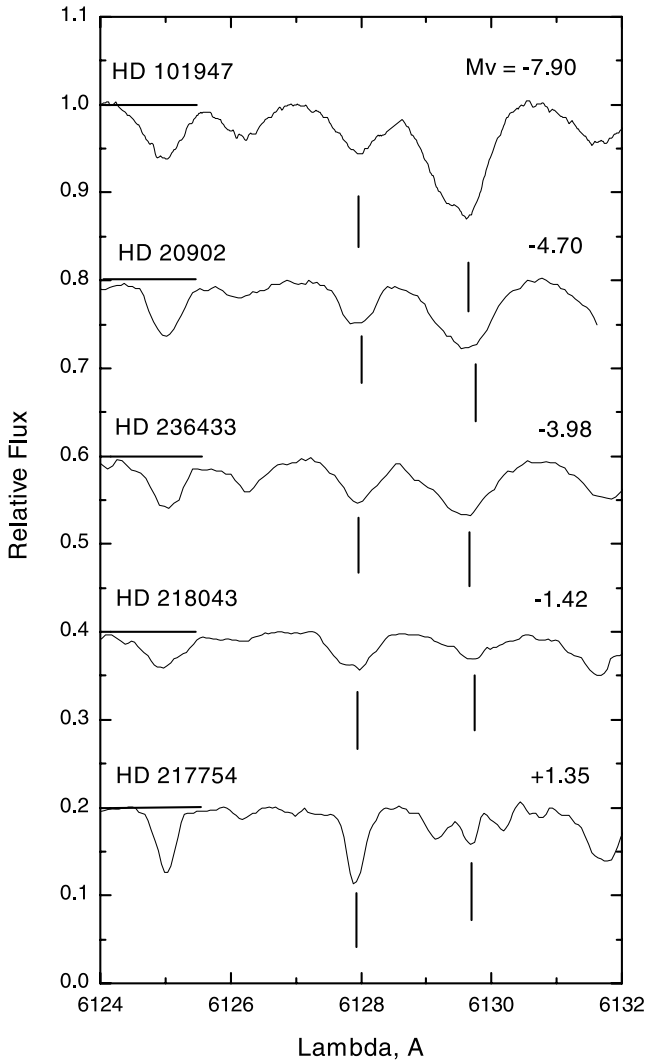
★ E-mail: val@deneb1.odessa.ua

Figure 1. Behaviour of the lines 6129.69 Fe II and 6127.91 Fe I on the absolute magnitude M_v for stars with $T_{eff} \approx 6400$–6600 K. Note that HD 217754 is a giant that falls outside the range of our calibration. It is shown to illustrate the behaviour of the lines at lower absolute magnitude.

is determined effectively by the strength of the Fe II lines, as the strength of the Fe I lines remains roughly constant. In more luminous objects, Fe II lines are expected to be stronger because of the higher ionization fraction, and to a lesser degree because of non-local thermodynamic equilibrium (NLTE) effects. The ratio, although relatively insensitive to temperature, is however a strong function of the absolute magnitude, as shown in Fig. 1. We observe similar correlations for other ion combinations, such as Si II/Si I, Cr II/Cr I, Fe II/Si I, Ba II/Fe I, etc.

In this paper, we explore this dependence in detail. We have chosen to restrict ourselves to Fe lines because these lines are the most numerous in F–G supergiants. In considering only Fe, we avoid allowing for elemental abundance variations between the stars. It should be noted that this spectral method is reddening-independent.

2 PROGRAMME SPECTRA

The spectra of the F–G supergiants investigated here were obtained using the 1.93-m telescope of the Haute-Provence Observatoire (France) equipped with the echelle spectrograph ELODIE (Baranne

et al. 1996). We retrieved them from the ELODIE on-line archive (Moultaka et al. 2004). The spectra have a resolving power $R = 42\,000$, cover the wavelength region 4400–6800 Å, and have a S/N ratio >100 at 5500 Å. The initial processing of the spectra (image extraction, cosmic ray removal, flat-fielding, etc.) was carried out as described in Katz et al. (1998).

For the classical Cepheid observations, we used the Sandiford Cassegrain Echelle Spectrograph (McCarthy et al. 1993) attached to the 2.1-m telescope at the McDonald Observatory. The spectra continuously cover a wavelength range from approximately 5600 to 7000 Å with a resolving power of about 60 000. Typical S/N values per pixel for the spectra are in excess of 150. IRAF[1] was used to perform CCD processing, scattered light subtraction and echelle order extraction.

We complemented these data sets with spectra obtained with the Ultraviolet-Visual Echelle Spectrograph (UVES) on the Very Large Telescope (VLT) Unit 2 Kueyen (Bagnulo et al. 2003). These observations were carried out in two instrumental modes, Dichroic1 (DIC1) and Dichroic2 (DIC2), in order to provide an almost complete coverage in the wavelength interval 3000–10 000 Å. The spectral resolution is about 80 000, and the typical S/N ratio is 300–500 in the V band.

For classical Cepheids, we have used the physical parameters determined in our previous studies (Andrievsky et al. 2002a,b,c; Luck et al. 2003, 2008; Andrievsky, Luck & Kovtyukh 2005; Kovtyukh et al. 2005; Luck & Andrievsky 2004; Luck, Kovtyukh & Andrievsky 2006). We have restricted the pulsation phases to those near maximum radius (phase about 0.4 and where the pulsation radial velocity $V_{rad} = 0\,km\,s^{-1}$) in order to minimize the contribution of the 'dynamical' term in the luminosity indicators. At the phase of maximum compression, strong thermal and dynamical effects (e.g. shock waves) are predicted to develop in Cepheid atmospheres, while phases near maximum radius may be considered relatively quiet, enabling us to better correlate the Cepheid's M_v with the spectral luminosity indicators. This is also near $\langle V \rangle$, which is the value used with the PL M_v to yield distances. This further means that the derived M_v relations when applied to Cepheids should yield a PL that is close to the standard Cepheid PL, assuming that we use the M_v obtained for the Cepheid at phase 0.4. This does ignore the difference in an intensity weighted mean V and a simple mean V. The difference is irrelevant at this level of accuracy.

Further processing – continuum placement, measurement of line depths and equivalent widths (EWs) – was carried out using the DECH20 package (Galazutdinov 1992). Line depths R_λ were measured by means of Gaussian fitting.

3 SELECTION OF THE CALIBRATING ABSOLUTE MAGNITUDES AND EFFECTIVE TEMPERATURES

The first step, and perhaps the most difficult, is to build a sample of supergiants with known absolute magnitudes M_v. This is a very important procedure as it affects the accuracy of the final luminosity scale, in particular the run of the systematic error with M_v and T_{eff}. For the 40 supergiants in our calibration sample (see Table 1), we took the bulk of the M_v estimates from Arellano Ferro & Parrao

---

[1] IRAF is distributed by the National Optical Astronomy Observatories, which are operated by the Association of Universities for Research in Astronomy, Inc., under cooperative agreement with the National Science Foundation.

Table 1. Calibrator non-variable supergiants and supergiants with computed M_v.

Star	Sp	M_v (reference)	T_{eff}	M_v	σ	N	s.e.	Comments
HD000371	G3II		5085	−2.30	0.23	10	0.07	
HD000611	G2Ib-II		5453	−2.50	0.32	67	0.04	doub
HD000725	F5Ib-II		6793	−4.97	0.50	68	0.06	
HD003421	G2.5IIa	−1.62(5)	5302	−1.38	0.25	64	0.03	
HD004362	G0Ib		5325	−3.07	0.29	70	0.04	
HD004482	G8II	0.98(5)	4874	0.47	0.34	6	0.14	
HD008906	F3Ib		6710	−4.68	0.42	69	0.05	
HD008992	F6Ib		6278	−3.60	0.24	38	0.04	
HD009973	F5Iab		6654	−5.08	0.43	40	0.07	Emiss
HD010494	F5Ia	−7.34(1)	6672	−7.42	0.37	44	0.06	NGC 654
HD011544	G2Ib	−6.62(2)	5123	−3.28	0.23	36	0.04	h&χ Per(?), non-member
HD016901	G0Ib-II	−3.25(6)	5555	−3.05	0.11	66	0.01	NGC 1039(?)
HD017971	F5Ia	−6.58(1)	6883	−6.56	0.30	61	0.04	IC 1848
HD018391	G0Ia	−7.76(4)	5846	−7.54	0.44	20	0.10	Anonymous cluster
HD020123	G6Ib-II	−1.64(6), −2.06(5)	5160	−1.84	0.55	38	0.09	Melotte 20, SB
HD020902	F5Iab:	−4.70(1), −4.13(5)	6550	−4.31	0.26	68	0.03	IC 4665, Var
HD026630	G0Ib	−3.20(5)	5309	−3.17	0.13	40	0.02	SB
HD031910	G1Ib-II	−3.29(5)	5423	−3.09	0.21	56	0.03	double
HD032655	F2II-III		6653	−3.05	0.53	50	0.07	
HD034248	G5		6101	−4.02	0.71	66	0.09	
hd036079	G5II	−0.49(5)	5184	−0.27	0.37	60	0.05	
HD036891	G3Ib		5082	−2.79	0.45	63	0.06	
HD038808	G3Ib-II		5112	−1.36	0.51	35	0.09	
HD039949	G2Ib		5248	−2.65	0.37	70	0.04	
HD042454	G2Ib		5277	−3.64	0.29	59	0.04	
HD044812	G5Ib		4896	−2.07	0.27	9	0.09	
HD047731	G5Ib		4989	−2.45	0.26	21	0.06	doub
HD048616	F5Ib		6413	−3.89	0.32	51	0.04	
HD052220	G1Ib		5661	−3.01	0.24	72	0.03	
HD053003	G0Ib		5540	−3.01	0.20	40	0.03	
HD057146	G2Ib		5134	−3.11	0.33	68	0.04	doub
HD058526	G3Ib		5287	−3.02	0.19	68	0.02	
HD062345	G8IIIa	0.54(5)	4971	0.48	0.17	16	0.04	doub
HD065228	F7/F8II	−1.87(5)	5740	−2.34	0.34	61	0.04	
HD067594	G2Ib		5187	−2.77	0.20	42	0.03	
HD074395	G1Ib	−2.27(5)	5264	−2.77	0.19	68	0.02	
HD074739	G8Iab:	−0.83(5)	4954	−0.79	0.28	17	0.07	
HD075276	F2Iab	−6.45(1)	6934	−6.44	0.17	45	0.03	Vel OB1
HD077020	G9II		4880	−0.72	0.08	8	0.03	
HD077912	G8Iab:	−2.51(5)	4957	−1.73	0.41	32	0.07	Pecul
HD079698	G6II	−0.15(5)	5252	−0.61	0.33	47	0.05	
HD084441	G1II	−1.28(5)	5296	−1.64	0.37	69	0.04	Var
HD090452	F3Ib		6688	−5.16	0.42	58	0.06	
HD092125	G2.5IIa	−1.52(5)	5354	−1.84	0.23	57	0.03	
HD099648	G8Iab:	−1.07(5)	4942	−0.60	0.31	24	0.06	doub
HD101947	F9Ia	−7.90(1)	6578	−7.28	0.35	35	0.06	Stock 14, V810 Cen
HD109379	G5II	−0.44(5)	5117	−0.57	0.25	35	0.04	Var
HD125809	G5/G6Ib		4837	−3.03	0.19	9	0.06	
HD136537	G2II		4960	−2.99	0.15	22	0.03	
HD139862	G7.5IIIaCNe...		5091	−0.38	0.31	9	0.10	
HD146143	F9Ia		6077	−3.62	0.22	42	0.03	
HD159181	G2Iab:	−2.71(5)	5198	−2.49	0.22	67	0.03	
HD164136	F2II	−2.85(5)	6483	−2.32	0.51	46	0.08	
HD171237	F2II		6792	−3.58	0.45	18	0.11	
HD171635	F7Ib		6201	−3.58	0.28	71	0.03	
HD172365	F8Ib-II	−2.50(2)	6117	−2.49	0.79	30	0.14	IC 4756
HD178524	F2II/III	−3.00(5)	6710	−3.04	0.33	55	0.04	doub
HD180028	F6Ib		6240	−3.23	0.30	35	0.05	
HD182296	G3Ib		5072	−3.15	0.40	27	0.08	
HD182835	F2Iab:		6912	−5.58	0.53	66	0.07	
HD183864	G2Ib		5323	−2.93	0.31	47	0.05	SB
HD185018	G0Ib		5451	−2.25	0.38	11	0.11	

Table 1 – *continued*

Star	Sp	M_v (reference)	T_{eff}	M_v	σ	N	s.e.	Comments
HD185758	G1II	−1.19(5)	5390	−1.21	0.27	43	0.04	
HD187203	F8Ib-II		5710	−3.16	0.31	25	0.06	post-AGB?
HD190323	G0Ia		6222	−4.45	0.21	72	0.02	
HD190403	G5Ib-II		4894	−1.83	0.23	9	0.08	
HD191010	G3Ib		5269	−1.40	0.36	55	0.05	Var
HD192713	G2Iab:		5028	−3.24	0.54	16	0.14	Algol
HD193370	F5Ib		6369	−3.80	0.25	67	0.03	SB
HD194093	F8Iab:	−5.5(1)	6202	−4.35	0.31	56	0.04	Var
HD195295	F5Iab:	−2.76(5)	6575	−3.32	0.41	61	0.05	Var
HD195432	G0II		5872	−2.07	0.56	38	0.09	
HD195593	F5Iab		6452	−4.83	0.19	6	0.08	
HD200102	G1Ib		5361	−2.43	0.23	57	0.03	
HD200805	F5Ib		6865	−4.58	0.49	52	0.07	
HD202109	G8III	0.16(5)	4976	0.12	0.27	33	0.05	
HD202314	G6Ib-II...		5004	−1.59	0.40	16	0.10	
HD204022	G0Ib		5375	−3.80	0.21	69	0.03	
HD204075	G4Ibp...	−2.05(5)	5287	−1.58	0.40	30	0.07	SB
HD204867	G0Ib	−3.09(5)	5431	−3.42	0.27	53	0.04	
HD205114	G2Ib+...		5224	−2.66	0.33	46	0.05	SB
HD206731	G8II		5030	−1.55	0.79	20	0.18	
HD206859	G5Ib	−2.79(5)	4876	−2.33	0.17	9	0.06	Var
HD207489	F5Ib		6350	−3.41	0.25	70	0.03	
HD209750	G2Ib	−2.98(5)	5199	−3.18	0.24	65	0.03	
HD214567	G8II	0.69(5)	4918	0.61	0.33	14	0.09	
HD214714	G3Ib-IICNe		5424	−0.92	0.58	49	0.08	
HD215665	G8Iab:	−1.14(5)	4848	−1.07	0.13	12	0.04	
HD216206	G4Ib		5003	−2.23	0.33	35	0.06	
HD219135	G0Ib		5479	−3.06	0.27	63	0.03	
HD220102	F2II		6832	−4.03	0.62	77	0.07	SB
HD223047	G5Ib+...		4808	−3.04	0.24	11	0.07	doub
HD224165	G8Ib		4804	−2.31	0.27	7	0.10	
HD236433	F4II	−3.98(3)	6541	−3.91	0.29	59	0.04	NGC 129, SB
HD249750	G5		5475	−2.97	0.58	46	0.09	
BD+60 2532	F7Ib	−4.10(2)	6268	−3.69	0.30	17	0.07	NGC 7654, doub

References are: (1) Arellano Ferro et al. (2003); (2) Arellano Ferro & Parrao (1990); (3) Slowik & Peterson (1995); (4) Turner et al. (2009); (5) from Hipparcos parallaxes, this paper; (6) from clusters, this paper.

(1990), Slowik & Peterson (1995) and Arellano Ferro et al. (2003). In addition, we included HD 18391, a member of an anonymous open cluster. Turner et al. (2009) estimate $E(B–V) = 1.10 \pm 0.02$ and a distance of 1661 ± 73 pc for this cluster, and thus $M_v = −7.76$. HD 16901 is a possible member of the open cluster NGC 1039 (M34) (Wachmann 1939). Kharchenko et al. (2005) estimate $E(B–V) = 0.07$ and $V–M_v = 8.71$ for the cluster, leading to $M_v = −3.25$ for HD 16901. We have also included field stars with precise *Hipparcos* parallaxes (M_v error less than 0.1 mag; van Leeuwen 2007). For the M_v determination of these stars, we used the $E(B – V)$ calibration from Kovtyukh et al. (2008). To this sample we added 39 classical Cepheids from our previous work (Table 2; M_v are from Fouque et al. 2007 and Feast 1999). The so-called s-Cepheids (Cepheids with sinusoidal light curves and small amplitudes) are first overtone pulsators. Microlensing surveys (MACHO and EROS) have unambiguously shown that all s-Cepheids pulsate in the first (or second) overtone (Beaulieu et al. 1995). V473 Lyr is a probable second overtone pulsator (Burki et al. 1986).

To improve the accuracy of the spectroscopic luminosity determination, precise T_{eff} are needed. The effective temperatures have been determined using the line ratio calibrations from Kovtyukh (2007). The internal accuracy of these estimates is particularly high in the temperature range 4800–6500 K, typically 150 K or less for the standard deviation, which translates to 10–20 K in the standard error. Another advantage of the line ratio method (or any other spectroscopic method) is that it is reddening-independent.

4 CALIBRATIONS

Fe II/Fe I line pairs were fitted against M_v and T_{eff} using a relation of the form

$$M_V = a + br + cr^2 + dr^3 + et + ft^2 + grt,$$

where $t = \log(T_{eff}) − 3.65$ and $r = R_{\lambda 1}/R_{\lambda 2}$. The coefficients a, b, c, d, e, f and g have been determined using standard least-squares methods; their formal errors are 0.25–0.80 mag (see, for example, Figs 2 and 3). We have assumed that all M_v are of the same accuracy. However, prior to the final least-squares fits, we excluded a few outlying values of M_v. These outliers included HD 11544 and HD 194093 (see Fig. 4). From the 459 Fe II/Fe I ratios examined, we have selected 80 combinations having a rms error in the individual fit smaller than 0.35 mag.

The M_v recovered from these 80 expressions are in excellent agreement with the original values, as shown in Fig. 4. The standard deviation is 0.26 mag, which we feel is the overall uncertainty in M_v derived using this calibration. The applicable range of the calibration is F2 to G8 ($T_{eff} = 7000$–4800 K), and for luminosity classes I and II ($M_v = −0.5$ to −8 mag).

Table 2. Calibrator Cepheids and Cepheids with computed M_v.

Star	P (d)	M_v PL relation	Phase	T_{eff} (K)	M_v (computed)	σ	N	s.e.	Comments
V473 Lyr	1.4908		0.383	6051	−2.35	0.45	71	0.05	2nd overtone
FI Mon	3.2878		0.355	5923	−2.48	0.32	35	0.05	
BG Cru	3.3427		0.283	6103	−2.98	0.42	30	0.08	s-Cep
SU Cas	1.9493	−2.45	0.405	6165	−2.82	0.23	72	0.03	2nd overtone, associat
DT Cyg	2.4991	−2.74	0.410	6017	−2.85	0.13	62	0.02	s-Cep
RT Aur	3.7282	−2.81	0.377	5878	−2.74	0.33	78	0.04	
SU Cyg	3.8455	−2.84	0.415	5956	−2.82	0.17	49	0.02	
AE Tau	3.8964		0.377	5941	−2.70	0.34	72	0.04	
α UMi	3.9696	−3.29	0.410	6057	−2.98	0.09	60	0.02	
SZ Tau	3.1484	−3.01	0.430	5901	−2.88	0.22	36	0.04	s-Cep
T Vul	4.4355	−3.01	0.431	5733	−3.06	0.14	46	0.02	
T Vel	4.6398		0.441	5564	−3.13	0.18	76	0.02	
V1334 Cyg	3.3330	−3.07	0.365	6159	−3.22	0.29	51	0.04	s-Cep
VZ Cyg	4.8644		0.361	5672	−3.11	0.16	67	0.02	
CF Cas	4.8752	−3.12	0.448:	5523	−3.45	0.61	41	0.09	NGC 7790
δ Cep	5.3663	−3.22	0.432	5640	−3.20	0.17	74	0.02	
Y Sgr	5.7734	−3.31	0.319	5733	−3.37	0.12	49	0.02	
FM Aql	6.1142	−3.38	0.437	5613	−3.48	0.33	44	0.05	
FF Aql	4.4709		0.437	6021	−3.24	0.15	59	0.02	s-Cep
X Vul	6.3195	−3.42	0.407	5649	−3.42	0.15	63	0.02	
AW Per	6.4636	−3.45	0.451	5879	−3.47	0.34	45	0.05	
U Sgr	6.7452	−3.50	0.480	5425	−3.50	0.23	23	0.05	cluster
η Aql	7.1767	−3.56	0.535	5426	−3.47	0.13	73	0.02	
V440 Per	7.5700	−3.63	0.376	6067	−3.43	0.15	75	0.02	
W Sgr	7.5949	−3.63	0.462	5540	−3.34	0.08	55	0.01	
VY Cyg	7.8570		0.368	5723	−3.37	0.21	67	0.03	
RX Cam	7.9120	−3.68	0.499	5464	−3.72	0.18	57	0.02	
W Gem	7.9138	−3.68	0.524	5483	−3.61	0.13	51	0.02	
U Vul	7.9906	−3.69	0.536	5525	−3.69	0.15	62	0.02	
DL Cas	8.0007	−3.69	0.353	5604	−3.59	0.23	57	0.03	cluster
V636 Cas	8.3770	−3.75	0.391	5426	−3.56	0.18	70	0.02	
S Sge	8.3821	−3.75	0.507	5406	−3.84	0.13	65	0.02	
V500 Sco	9.3168	−3.87	0.401	5300	−4.12	0.23	50	0.03	
FN Aql	9.4816	−3.89	0.394	5239	−3.99	0.17	62	0.02	
SX Vel	9.5499		0.354	5594	−3.87	0.16	61	0.02	
ζ Gem	10.1507	−3.97	0.416	5225	−3.89	0.13	49	0.02	
Z Lac	10.8856	−4.06	0.412	5281	−4.24	0.13	57	0.02	
VX Per	10.8890	−4.06	0.210	5279	−4.08	0.23	64	0.03	
VY Sgr	13.5572		0.394	5069	−4.82	0.31	53	0.04	
BN Pup	13.6731		0.396	5141	−4.48	0.20	49	0.03	
TT Aql	13.7547	−4.33	0.328	5404	−4.26	0.16	68	0.02	
SV Mon	15.2328	−4.44	0.352	5204	−4.62	0.12	44	0.02	
X Cyg	16.3863	−4.53	0.377	5022	−4.75	0.15	38	0.02	
RW Cam	16.4148	−4.53	0.328	5183	−4.39	0.14	55	0.02	
CD Cyg	17.0740	−4.58	0.434	5194	−4.41	0.10	50	0.01	
Y Oph	17.1269		0.454	5561	−3.90	0.15	60	0.02	
SZ Aql	17.1408	−4.58	0.402	5231	−4.59	0.19	45	0.03	
VX Cyg	20.1334		0.410	5087	−4.53	0.22	61	0.03	
WZ Sgr	21.8498	−4.86	0.334	5099	−4.92	0.27	49	0.04	cluster
BM Per	22.9519		0.350	5345	−4.71	0.24	61	0.03	
SW Vel	23.4410	−4.95	0.419	5088	−4.91	0.19	30	0.03	associat
T Mon	27.0246	−5.11	0.358	5020	−5.10	0.21	46	0.03	associat
SV Vul	44.9948	−5.70	0.414	5000	−5.46	0.21	52	0.03	

Table 3 provides the fit coefficients for 18 typical calibrations, together with the wavelengths (λ_1, λ_2) and the excitation potentials (EPLs; in eV) for the corresponding lines, as well as the applicable temperature range. The remaining 62 calibrations are available in electronic form from the author VVK upon request.

We then applied these calibrations to compute M_v for a sample of 96 F–G supergiants and 53 Cepheids. The results are given in Tables 1 and 2. Each entry includes the name of the star, M_v from the literature, T_{eff}, mean M_v, error (σ), number of calibrations used (N) and the standard error (s.e.).

For some of the line pairs in Table 3, the coefficients e, f and g are missing, indicating no temperature dependence (for given temperature and M_v region only). An Fe II/Fe I ratio is not only a function of the EPLs of the lower levels, but is also a function
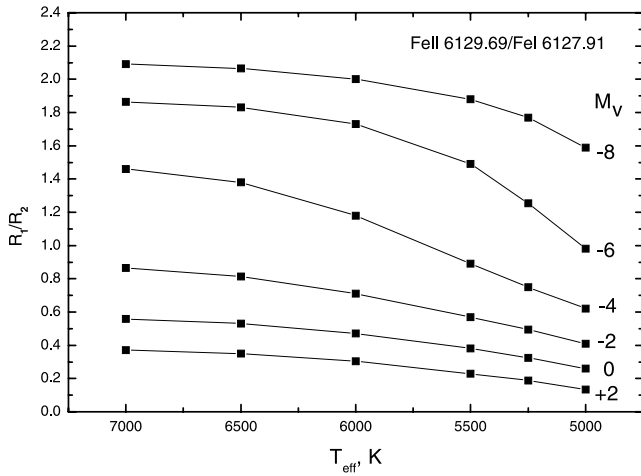
Figure 2. Calibration of the ratio 6129.69 Fe II/6127.91 Fe I on the absolute magnitude M_v and the effective temperature T_{eff} (EPL = 3.20 and 4.14 eV, respectively).
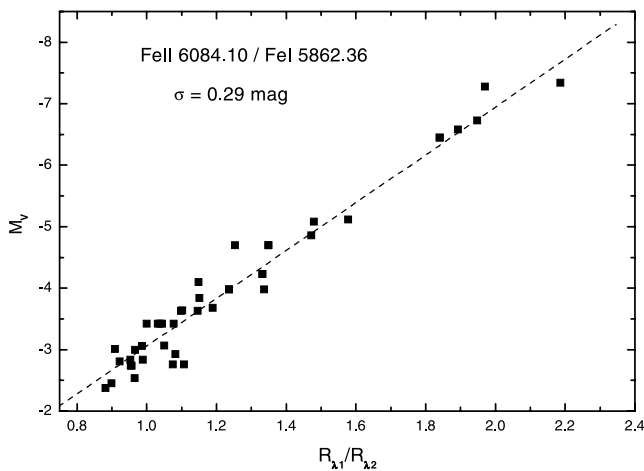

Figure 3. Example of linear calibration between the ratio 6084.10 Fe II/5862.36 Fe I and the absolute magnitude M_v ($5800 < T_{eff} < 7000$ K; EPL = 3.20 and 4.55 eV, respectively).

of the ionization potentials of Fe I and Fe II. As pointed out by Lyubimkov & Boyarchuk (1983) and Rentzsch-Holm (1996), the NLTE effects for Fe I lines are very pronounced and depend upon the EW. According to Lyubimkov & Boyarchuk (1983), the NLTE corrections to the iron abundance in F0 supergiants reach about 0.6 dex when using lines with EW = 200 mÅ, and 0.1–0.2 dex in the case of lines having EW = 50 mÅ. Note that LTE results for lines of 200 mÅ are especially sensitive to both the microturbulence assumed and the model atmosphere structure providing the LTE abundance result. At the same time, Fe II lines are not particularly sensitive to departures from LTE. Severe overionization of Fe II is unlikely in F–G supergiants, while for Fe I atoms it can be expected, as first pointed out by Auman & Woodrow (1975). This conclusion was confirmed by statistical equilibrium calculations for Fe II/Fe I in the atmosphere of late-type stars (Th évenin & Idiart 1999). It appears that all of these difficulties can combine to obviate the expected dependence of the Fe II/Fe I ratio on temperature.

The averaging of 50–75 M_v values for an individual star, as derived from a like number of line ratios, significantly reduces the uncertainty in the final M_v. The final formal precision achieved is 0.03–0.25 mag (one standard error of the mean) for spectra of $R =$
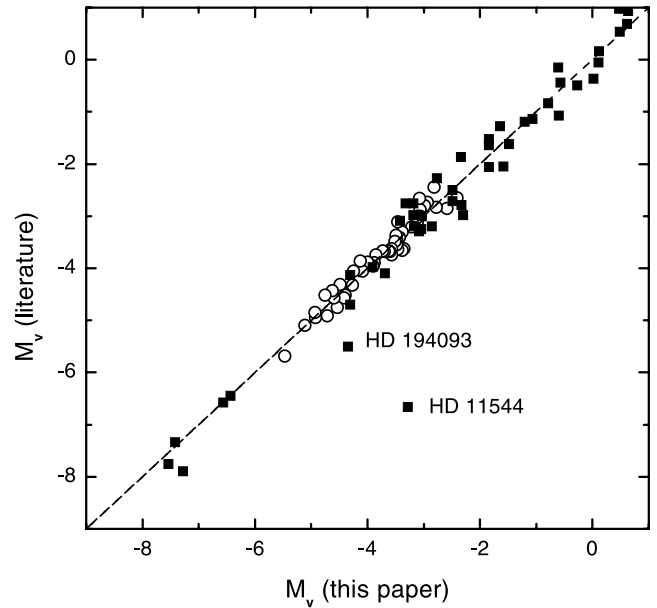

Figure 4. Comparison of our final M_v from several calibrations with the estimates from the literature. Classical Cepheids are plotted as open circles, and supergiants as filled squares. The supergiants HD 11544 and HD 194093 deviate from the least-squares fit found for the remaining F–G supergiants.

40 000, S/N = 100–150 and $v \sin i < 30$ km s^{-1}. Better precision can be achieved using higher S/N spectra (note that the lines in a typical supergiant are fully resolved at $R = 30\,000$, so better resolution will not increase the precision). We note that this error budget does not include possible uncertainties arising from the individual properties of stars, such as rotation, chemical composition, binarity, etc.

The calibrations have been also applied to the Cepheid δ Cep (Fig. 5). The 'observed' M_v values are based on a distance of 249 pc (Gieren, Fouque & Gomez 1998), a reddening of 0.092 (Kovtyukh et al. 2008) and the photometry of Moffett & Barnes (1984). We see that phases near maximum radius ($\phi \approx 0.4$) provide accurate M_v determinations. However, for phases between minimum and maximum light (roughly minimum radius) the calibration yields absolute magnitudes as much as 0.8 mag from the expected value. It is interesting to note that the spectroscopic parameter (log g, V_t, [Fe/H]) and abundance determinations at those phases (Andrievsky et al. 2005) reveal no untoward behaviour.

We have also compared our M_v with the PL relations by Gieren et al. (1998) and Fouque et al. (2007). This is shown in Fig. 6. The agreement is quite good. Only Y Oph shows an anomalous position in these relations. Note that the unusual Cepheid Y Oph has shown a decline in light amplitude during the twentieth century (Fernie, Khoshnevissan & Seager 1995) and an anomalous light curve for its period (see also Luck et al. 2008).

We thus confirm that the Fe II/Fe I line ratio is a good luminosity indicator.

5 HERTZSPRUNG–RUSSELL DIAGRAM

We use our newly derived values of M_v to construct an H–R diagram for luminous stars. Observationally, F–G supergiants are rare stars as they represent a relatively brief phase in the evolution of intermediate mass stars, typically a few Myr, or about 10 per cent of their total lifetime. These supergiants are core He burners in

Table 3. The 18 typical M_v calibrations ($M_V = a + br + cr^2 + dr^3 + et + ft^2 + grt$).

λ (Fe II) (Å)	EPL (eV)	λ (Fe I) (Å)	EPL (eV)	a	b	c	d	e	f	g	σ (K)	$\Delta T_{\rm eff}$ (K)
5725.96	3.42	5852.19	4.55	−10.711	8.705	–	–	66.490	–	−78.866	0.29	5800–7000
5732.71	3.39	5809.25	3.88	4.752	−55.328	78.708	−39.778	68.864	−179.319	–	0.28	4900–6600
5823.15	5.57	6240.66	2.22	−2.039	–	–	–	–	–	−16.065	0.32	5800–7000
5824.41	3.42	5752.01	4.55	−0.576	−108.854	419.043	−542.766	100.487	−402.582	–	0.34	5000–7000
5991.37	3.15	6024.07	4.55	1.376	−6.799	–	–	17.250	–	–	0.35	5800–7000
6084.10	3.20	5862.36	4.55	0.832	−3.889	–	–	–	–	–	0.29	5800–7000
6113.33	3.22	6007.96	4.65	6.976	−35.191	26.545	−7.602	74.760	−173.858	–	0.27	5000–6600
6129.69	3.20	6127.91	4.14	2.159	−21.728	14.889	−3.926	58.706	−142.434	–	0.30	4900–6600
6179.39	5.57	5987.05	4.80	−2.570	−43.046	68.664	−48.828	92.688	−204.166	–	0.27	5000–6600
6233.53	5.48	6806.85	2.73	−12.379	−2.182	–	–	84.428	–	–	0.29	5800–7000
6239.91	3.89	5862.36	4.55	−0.589	−5.704	–	–	14.140	–	–	0.29	5800–7000
6239.91	3.89	6232.65	3.65	5.653	−36.308	30.504	−10.214	49.890	–	–	0.28	5000–6600
6248.89	5.51	5753.12	4.26	1.094	−13.080	–	–	-14.750	–	47.812	0.30	5800–7000
6369.46	2.89	6419.98	4.73	7.846	−10.942	–	–	-32.876	–	36.096	0.26	5800–7000
6383.72	5.55	6419.98	4.73	13.046	−108.273	220.614	−158.932	–	181.224	–	0.28	5100–6400
6432.68	2.89	6024.07	4.55	2.059	−6.972	–	–	19.197	–	–	0.29	5800–7000
6442.94	5.55	6330.86	4.73	−4.434	−20.257	12.964	−2.728	154.938	−532.195	–	0.29	5000–6600
6446.40	6.22	5762.99	4.21	−6.448	–	–	–	40.857	–	−63.274	0.31	5800–7000
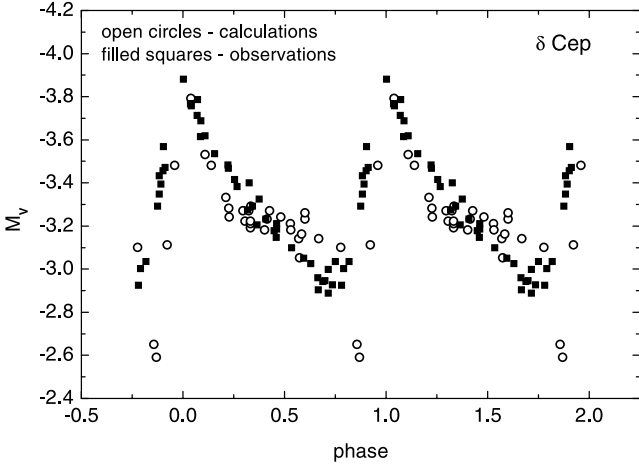
Figure 5. Comparison of our spectroscopically determined M_v with M_v from the light curve for the classical Cepheid δ Cep: filled squares, observations; open circles, calculations (individual phases for the Cepheid are shown).
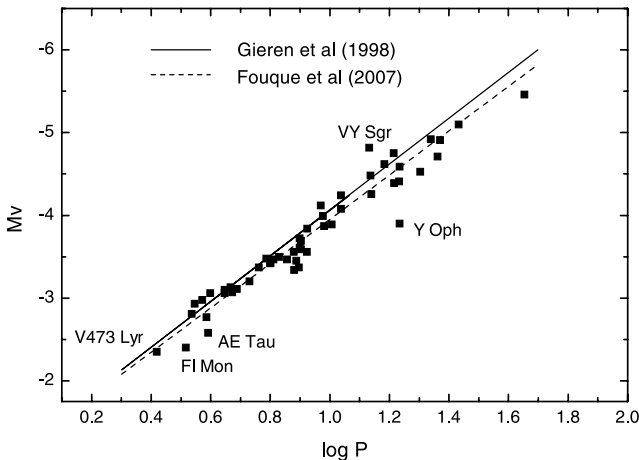
Figure 6. Comparison of our M_v with PL relations for the Cepheids.

all probability. From the work of Salasnich et al. (2000) for 10 solar masses at $Z = 0.07$ (alpha-enhanced), the H lifetime is 1.27×10^7 yr and the He time is 1.62×10^6 yr. The He phase is 12 per cent of the H time or 11 per cent of the total. Going down to $Z = 0.008$ (solar alpha), the lifetimes increase but the He-burning phase fraction remains at about 10 per cent of the total lifetime. The Schaller solar metallicity tracks (Schaller et al. 1992, see table 45) also give the pertinent set of lifetimes. The He phase is about 10 per cent of the lifetime and is 1.6 (nine solar masses) to 2.6 (12 solar masses) Myr. The rarity of supergiants depends on how we look at the fractions of differing mass stars. With respect to standard initial mass functions (IMFs), about 10 per cent of stars have these masses. However, as their lifetimes are short, they are a small part of the total number stars accumulated over the history of the Galaxy. Their numbers and location on the H–R diagram are also difficult to predict theoretically, as models are very sensitive to the uncertain values of the mass-loss rate and the treatment of mixing.

The loci of the luminous stars on the H–R diagram are shown in Fig. 7. The two dashed vertical lines denote the yellow supergiant region, which we define as having effective temperatures between 4800 and 7000 K. Evolutionary tracks from Salasnich et al. (2000) for $Z = 0.019$ and $[\alpha/Fe] = 0$ are shown for reference. These models do not develop long blue loops for stars with 2–5 M$_\odot$, and hence they do not cross the instability strip. However, stars with 5–7 M$_\odot$ do show blue loops that cross the lower part of the Cepheid instability strip.

In Fig. 7, we also show the location of our yellow supergiants and classical Cepheids in the H–R diagram. First, we find that the $Z = 0.019$ tracks do a good job of predicting the positions of the blue loops and yellow supergiants for $M_v > −5$. The most luminous yellow supergiants in our sample have $M_v \sim −8$, consistent with the evolutionary tracks.

The majority of stars from Table 1 with M_v in the range from −4 to −7 have definitely passed the red giant branch and populate the region of the blue loops of 7–12 M$_\odot$ models. Blue loops for higher masses are not populated, in part because of the limited sample considered, but also because evolution in this region of the diagram is very fast.
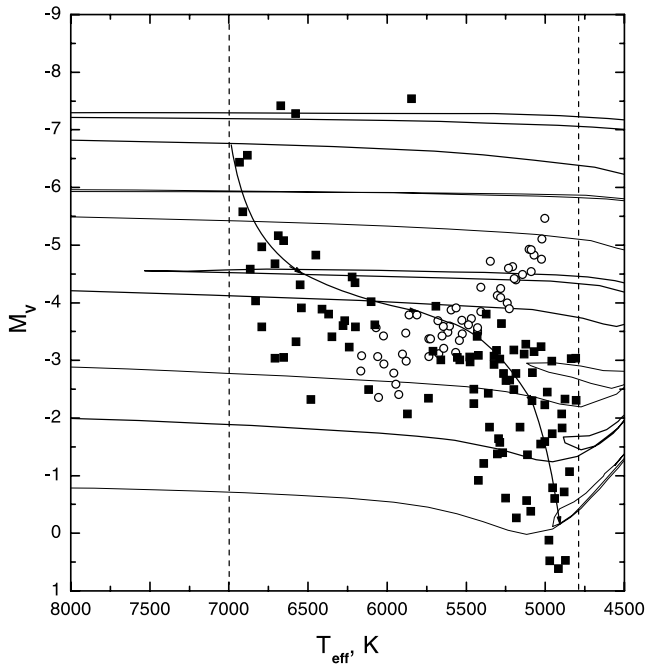
Figure 7. The H–R diagram constructed using our parameters. Classical Cepheids are plotted as open circles, supergiants as filled squares. Lines indicate evolutionary tracks by Salasnich et al. (2000) for 15, 10, 7, 5, 4 and 3 $M_\odot$ (top to bottom) for $z = 0.019$ and $[\alpha/Fe] = 0$. The thick line indicates the observed edge of blue loops.

6 SUMMARY AND CONCLUSION

We have shown that Fe II/Fe I line depth ratios can be used for the determination of the luminosity of classical Cepheids and non-variable yellow supergiants. Starting with M_v from the literature, we calibrated 80 selected line ratios in terms of M_v and T_{eff}. The new calibrations are valid for the luminosity classes Ia, Ib and II, and the spectral types F2–G8. The precision of the method is ± 0.26 mag, for stars within a wide range of M_v from -8.0 to -0.5 mag. We applied these calibrations to derive the absolute magnitudes of a sample of intermediate temperature supergiants and classical Cepheids (see Tables 1 and 2).

Based on the inferred parameters for our sample, we constructed an H–R diagram. The luminosities determined in the present work can help in the determination of the evolutionary status of individual stars. These stars must lie on the blue loops, and therefore the extent of their positions in the H–R diagram places constraints on the extension of the blue loops of the evolutionary tracks. A difficulty is that the lower mass evolutionary tracks do not have blue loops that penetrate the instability strip. However, the CNO abundances of short period Cepheids (Luck & Lambert 1985) indicate that they are post-first dredge up and thus have entered the instability strip from the red side.

ACKNOWLEDGMENTS

This work is based on spectra collected with the 1.93-m telescope of the Haute-Provence Observatoire (France), the 2.1-m Otto Struve Telescope of the McDonald Observatory of the University of Texas at Austin, and the ESO Telescopes at the Paranal Observatory un-

der programme ID266.D-5655. We also thank the referee, Tõnu Kipper, for his helpful comments. Much of the information about the supergiants was gathered with the help of SIMBAD.

REFERENCES

Andrievsky S. M., 1998a, AN, 319, 239
Andrievsky S. M., 1998b, IBVS, 4572, 1
Andrievsky S. M. et al., 2002a, A&A, 381, 32
Andrievsky S. M., Bersier D., Kovtyukh V. V., Luck R. E., Maciel W. J., Lepine J. R. D., Beletsky Yu. V., 2002b, A&A, 384, 140
Andrievsky S. M., Kovtyukh V. V., Luck R. E., Lepine J. R. D., Maciel W. J., Beletsky Yu. V., 2002c, A&A, 392, 491
Andrievsky S. M., Luck R. E., Kovtyukh V. V., 2005, AJ, 130, 1880
Arellano Ferro A., Parrao L., 1990, A&A, 239, 205
Arellano Ferro A., Mendoza V., Eugenio E., 1993, AJ, 106, 2516
Arellano Ferro A., Giridhar S., Rojo Arellano E., 2003, RevMexAA, 39, 3
Auman J. R., Woodrow J. E. J., 1975, ApJ, 197, 163
Bagnulo S. et al., 2003, ESO Messenger, 114, 10
Baranne A. et al., 1996, A&AS, 119, 373
Beaulieu J.-P. et al., 1995, A&A, 303, 137
Burki G., Schmidt E. G., Arellano Ferro A., Fernie J. D., Sasselov D., Simon N. R., Percy J. R., Szabados L., 1986, A&A, 168, 139
Feast M., 1999, PASP, 111, 775
Fernie J. D., Khoshnevissan M. H., Seager S., 1995, AJ, 110, 1326
Fouque P. et al., 2007, A&A, 476, 73
Galazutdinov G. A., 1992, Prepr. SAO RAS, 92, 28
Gieren W. P., Fouque P., Gomez M., 1998, ApJ, 496, 17
Gray D. F., 1992, The Observation and Analysis of Stellar Photospheres. Cambridge Univ. Press, Cambridge
Katz D., Soubiran C., Cayrel R., Adda M., Cautain R., 1998, A&A, 338, 151
Kharchenko N. V., Piskunov A. E., Röser S., Schilbach E., Scholz R.-D., 2005, A&A, 438, 1163
Kovtyukh V. V., 2007, MNRAS, 378, 617
Kovtyukh V. V., Andrievsky S. M., Belik S. I., Luck R. E., 2005, AJ, 129, 433
Kovtyukh V. V., Soubiran C., Luck R. E., Turner D. G., Belik S. I., Andrievsky S. M., Chekhonadskikh F. A., 2008, MNRAS, 389, 1336
Luck R. E., Andrievsky S. M., 2004, AJ, 128, 343
Luck R. E., Lambert D. L., 1985, ApJ, 298, 782
Luck R. E., Gieren W., Andrievsky S. M., Kovtyukh V. V., Fouqué P., Pont F., Kienzle F., 2003, A&A, 401, 939
Luck R. E., Kovtyukh V. V., Andrievsky S. M., 2006, AJ, 132, 902
Luck R. E., Andrievsky S. M., Fokin A., Kovtyukh V. V., 2008, AJ, 136, 98
Lyubimkov L. S., Boyarchuk A. A., 1983, Ap, 19, 385
McCarthy J. K., Sandiford B. A., Boyd D., Booth J. M., 1993, PASP, 105, 881
Moffett T. J., Barnes T. G., 1984, ApJS, 55, 389
Moultaka J., Ilovaisky S. A., Prugniel P., Soubiran C., 2004, PASP, 116, 693
Rentzsch-Holm I., 1996, A&A, 312, 966
Salasnich B., Girardi L., Weiss A., Chiosi C., 2000, A&A, 361, 1023
Schaller G., Schaerer D., Meynet G., Maeder A., 1992, A&AS, 96, 269
Slowik D. J., Peterson D. M., 1995, AJ, 109, 2193
Thévenin F., Idiart T. P., 1999, ApJ, 521, 753
Turner D. G., Kovtyukh V. V., Majaess D. J., Lane D. J., Moncrieff K. E., 2009, AN, 330, 807
van Leeuwen F., 2007, A&A, 474, 653
Wachmann A. A., 1939, Spektral-Durchm. Milchstr., Teil 1, 1, 0

This paper has been typeset from a TEX/LATEX file prepared by the author.